Prediction of two-dimensional diluted magnetic semiconductors: Doped monolayer MoS$_2$ systems

Y. C. Cheng,[1] Z. Y. Zhu,[1] W. B. Mi,[2] Z. B. Guo,[3] and U. Schwingenschlögl[1,*]

[1]*PSE Division, King Abdullah University of Science and Technology (KAUST), Thuwal 23955-6900, Kingdom of Saudi Arabia*

[2]*Tianjin Key Laboratory of Low Dimensional Materials Physics and Preparing Technology, Institute of Advanced Materials Physics,*
Faculty of Science, Tianjin University, Tianjin 300072, China

[3]*Core Labs, King Abdullah University of Science and Technology (KAUST), Thuwal 23955-6900, Kingdom of Saudi Arabia*

Using first-principles calculations, we propose a two-dimensional diluted magnetic semiconductor: monolayer MoS$_2$ doped by transition metals. Doping of transition metal atoms from the IIIB to VIB groups results in nonmagnetic states, since the number of valence electrons is smaller or equal to that of Mo. Doping of atoms from the VIIB to IIB groups becomes energetically less and less favorable. Magnetism is observed for Mn, Fe, Co, Zn, Cd, and Hg doping, while for the other dopants from these groups it is suppressed by Jahn-Teller distortions. Analysis of the binding energies and magnetic properties indicates that (Mo,X)S$_2$ (X = Mn, Fe, Co, and Zn) are promising systems to explore two-dimensional diluted magnetic semiconductors.

PACS number(s): 75.50.Pp, 73.22.−f, 75.75.−c

In the past years extensive investigations of diluted magnetic semiconductors (DMSs) have been performed, because of exciting effects in this materials class, such as exciton spin polarization and spin-polarized electrical current, which gives rise to potential applications in spintronics.[1,2] Research has focused on the transition metal (transition metal) doped III-V and II-VI three-dimensional (3D) semiconductors. On the other hand, two-dimensional (2D) materials have raised a lot of attention recently, in particular, since the discovery of graphene in 2004.[3] This also brought up the idea of 2D DMSs.[4,5] Though graphene has been considered as a promising host material for transition metal implantation,[6] the lack of a band gap hampers the control of the charge and magnetic states. It has been proposed that this difficulty can be overcome by the introduction of semiconducting layers, such as monolayer h-BN.[7] However, as a consequence of the single atom thickness of both graphene and h-BN as well as optimization of the bond length to the implanted transition metal atoms,[6,7] the latter will stick out of the plane of the host material, which leads to chemical instability if the system is exposed to air.

The semiconducting transition metal dichalcogenides MX_2 (M = Mo, W and X = S, Se) crystallize in a layered $2H$ prototype structure consisting of weakly van der Waals bonded X-M-X slabs. They are characterized by distinct electronic, optical, and catalytic properties.[8–10] The compounds are also useful for dry lubrication[11] and exhibit interesting valley physics.[12] Recently, monolayer MoS$_2$ (1.8 eV direct band gap) has been fabricated by micromechanical exfoliation,[13] liquid exfoliation,[14] and chemical vapor deposition.[15] In addition, monolayer MoS$_2$ transistors have been demonstrated with carrier mobilities of 200 cm^2 V^{-1} s^{-1} at room temperature (which is similar to that of graphene nanoribbons), current on/off ratios of 1×10^8, and ultralow standby power dissipation.[14] Because of the sandwich S-Mo-S structure [see Fig. 1(a)], the direct band gap of 1.8 eV, and the transition metal nature of Mo, we expect to obtain a 2D DMS by replacing Mo by other transition metal atoms to induce electron or hole doping and magnetism.

In this Rapid Communication, we present a systematic first-principles study of monolayer MoS$_2$ doped by transition metal atoms from periods four, five, and six. The relaxed

structures for dopants from the IIIB to VIB groups retain C_{3v} symmetry, while dopants from the VIIB to IIB groups (except for Mn, Fe, Co, Zn, Cd, and Hg) lead to a Jahn-Teller distortion. As a consequence, there is no magnetism in these systems. We propose that 2D DMSs are very likely to be realized in monolayer MoS$_2$ doped by Mn, Fe, Co, or Zn.

We address the electronic properties of doped monolayer MoS$_2$ using the QUANTUM ESPRESSO package in the framework of density functional theory.[16,17] Ultrasoft pseudopotentials[18] as well as the generalized gradient approximation in the Perdew-Burke-Ernzerhof parametrization[19] of the exchange correlation functional are employed. All simulations are carried out for a $4 \times 4 \times 1$ supercell with 16 Mo atoms and 32 S atoms. A 10 Å vacuum layer is adopted in our slab calculations to avoid interaction between the slabs.[20] By replacing one Mo atom with a transition metal atom, the impurity concentration is set to 6.25%. A high cutoff energy of 544 eV and a precise $4 \times 4 \times 1$ k-point sampling grid are used. For the self-consistency cycle we employ an energy criterion of 10^{-10} eV. The structural optimization is continued until the residual forces have converged to less than 2.6×10^{-3} eV/Å and the total energy to less than 1.4×10^{-4} eV. We also have adopted on-site Coulomb interactions ranging from 1 to 4 eV to study the effects on the structure and magnetic properties of Ni and Mn doped monolayer MoS$_2$. However, we find no relevant influence on our conclusions and therefore discuss in the following the results without on-site interaction.

Bulk MoS$_2$ has a layered $2H$ prototype structure with space group $P6_3mmc$ (D_{6h} point group), which consists of weakly van der Waals bonded S-Mo-S slabs, and an indirect band gap of 1.3 eV. The trigonal prismatic coordination of the bulk is maintained in monolayer MoS$_2$, whereas the symmetry is reduced to $P\bar{6}m2$ (D_{3h} point group) due to a loss of inversion symmetry. Figure 1(a) shows a side view of the atomic structure of monolayer MoS$_2$, which is a semiconductor with a direct band gap of 1.8 eV.[10,21,22] The valence band maximum and conduction band minimum are located at the K point of the Brillouin zone. The point group of monolayer MoS$_2$ with one Mo vacancy remains C_{3v} [see Fig. 1(b)]. The same applies to the replacement of one Mo atom by another transition metal atom [see Fig. 1(c)]. Under the structure relaxation the C_{3v}
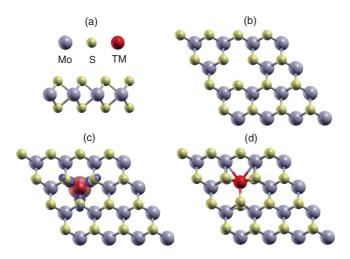
FIG. 1. (Color online) Monolayer MoS_2: (a) Side view, (b) top view with Mo vacancy, (c) spin density for Mn doping with C_{3v} symmetry, and (d) Ni doping with C_1 symmetry. Spin densities of $\pm 0.002 e$/bohr^{-3} are visualized by red and blue isosurfaces, respectively.

symmetry is maintained for dopants from the IIIB to VIB and IIB groups as well as Mn, Fe, and Co, whereas a Jahn-Teller distortion is observed otherwise.

Though the formation of a Mo vacancy requires more energy than that of a S vacancy, it has been reported that Co doping can be achieved at the MoS_2 edge by sulfidation of a mixture of ammonium heptamolybdate and cobalt nitrate,[23] which paves the way to transition metal doping by substitution of Mo in MoS_2. We have studied a zigzag MoS_2 nanoribbon with one S edge and one Mo edge to mimic the reported edge structure. Due to the dangling bonds at the edges, the nanoribbon turns out to be ferromagnetic with a total magnetic moment of $2.5\mu_B$ per cell. The moment reduces to $1.3\mu_B$ per cell under substitution of one Mo on the Mo edge by Co, which can be attributed to the coupling of the Co moment to the edge state.

Moreover, it has been demonstrated experimentally that pulsed laser deposition can be used to dope graphene by single transition metal atoms, such as Pt, Co, and In.[24] It is to be expected that the same approach can be applied to monolayer MoS_2 to realize single atom doping. To check the stability of different dopants, we have calculated the binding energies as summarized in Fig. 2. The binding energy is defined as $E_b = E_v + \mu - E_d$, where E_v is the energy of a relaxed MoS_2 monolayer with one Mo vacancy, μ is the energy of the doped transition metal atom, and E_d is the energy of a relaxed MoS_2 monolayer with one Mo atom replaced by the transition metal.

The value of E_b for different dopants varies strongly from 0.2 to 16.0 eV. Mo self-substitution yields the binding energy of a Mo atom, which is 13.5 eV. The three values of E_b shown in Fig. 2 for the IVB, VB, and VIB groups are similar, and larger than for the other groups. The binding energy increases with the period for the IVB, VB, VIB, VIII8, and VIII9 groups, while it decreases for the VIII10, IB, and IIB groups. We can conclude that substitutional doping of transition metal atoms from the IIIB to VIII10 groups is stable. Doping of transition metal atoms from the IB and IIB groups is difficult because of the low binding energies (especially for Hg). We find that monolayer MoS_2 doped by Mn, Fe, Co, Zn, Cd, or Hg is ferromagnetic. The magnetic moments are listed in Table I. The binding energies and magnetic moments indicate that Mn, Fe, Co, and Zn doping of monolayer MoS_2 are very promising approaches to achieve 2D DMSs. The origin of the magnetism for Mn, Fe, Co, Zn, Cd, and Hg doping as well as the absence of magnetism in the other cases will be discussed later.

The density of states (DOS) in Fig. 3(a) shows a band gap of 1.70 eV for the pristine monolayer MoS_2, which is only an underestimation of 0.10 eV as compared to the values obtained experimentally[10] and by GW calculations.[22] The tiny difference indicates the validity of the generalized gradient approximation for MoS_2. For S vacancies in MoS_2, Fig. 3(b) shows unoccupied shallow impurity states in the band gap near the conduction bands. In addition, the formation energy of a S vacancy is 6.0 eV, which is much less than that of a Mo vacancy (13.5 eV). In fact, it has been demonstrated that a S vacancy is easier formed under electron irradiation than a Mo vacancy.[25] This also demonstrated that the vacancies can be consecutively filled with other atomic species. For example, F, Cl, Br, and I can donate electrons to the MoS_2 and fill the unoccupied shallow impurity states near the conduction bands.[25] Both the electronic structure and formation energies indicate that the filling of a S vacancy with a donor atom induces free electrons in monolayer MoS_2.[13]

Before turning to MoS_2 doped by transition metal atoms, we next study the electronic structure of monolayer MoS_2 with one Mo vacancy. The structure maintains the C_{3v} symmetry [see Fig. 1(b)]. There are states in the band gap near the valence bands [see Fig. 3(c)]. The defect levels can be classified as a, e_1, and e_2 states due to a mixture of the S p orbitals. Each Mo vacancy can extract four electrons from the system, which results in p-type doping. Two electrons occupy the e_1 spin-up channel and two occupy the e_1 spin-down channel. Therefore, neither Mo vacancies nor S vacancies can introduce magnetism in MoS_2, which is different from the intrinsic magnetism in defective graphene and h-BN.[6,7,26]
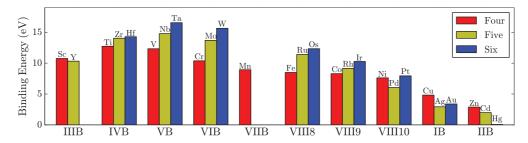

FIG. 2. (Color online) Binding energies of monolayer MoS_2 doped by transition metal atoms from the periods four, five, and six.

TABLE I. Magnetic moment, crystal field splitting Δ_{cf}, exchange splitting Δ_{ex}, magnetic energy $\Delta E = E_{FM} - E_{AFM}$, and Curie temperature T_C for $(Mo,X)S_2$ ($X = $ Mn, Fe, Co, Zn, Cd, and Hg) with 6.25% doping.

Magnetic moment (μ_B)		Δ_{cf} (meV)	Δ_{ex} (meV)	ΔE (meV)	T_C (K)
Mn	1.0	694	532	−0.02	0.2
Fe	2.0	704	650	3.92	
Co	3.0	412	515	1.38	
Zn	2.0	309	82	−3.30	38.3
Cd	2.0	367	91	−2.88	33.4
Hg	2.0	302	89	−1.85	21.5

With respect to the structure and calculated magnetism of $(Mo,X)S_2$, we classify the transition metals into three classes: IIIB to VIB groups, VII8 to IB groups, and the IIB group. We take Sc as a prototypical element from the first class. The symmetry of $(Mo,Sc)S_2$ is C_{3v} and the DOS shows spin degeneracy [see Fig. 3(d)]. An isolated Sc atom has a $3d4s^2$ configuration and three valence electrons less than Mo. The fact that the impurity states are close to the valence bands indicates p-type doping.

We study $(Mo,Mn)S_2$ as a prototypical example from the second class. Figure 3(e) shows spin polarization for this case. An isolated Mn atom has a $3d^54s^2$ configuration with one additional valence electron as compared to Mo. The impurity states are close to the conduction bands, which indicates n-type doping. The spin density isosurface in Fig. 1(c) illustrates that the magnetic moment is mainly due to the Mn atom. The Mn
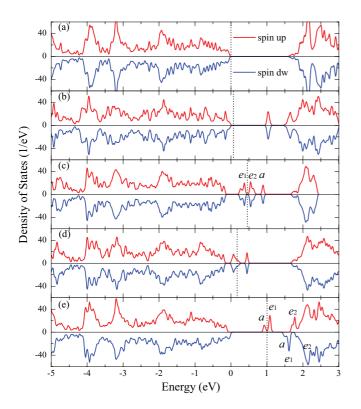
$3d$ orbitals are split into a single a (d_{z^2}) state and two twofold degenerate e_1 (d_{xy,x^2-y^2}) and e_2 ($d_{xz,yz}$) states, because of the C_{3v} symmetry. Six electrons occupy the valence states and the remaining the a spin-up defect state. The exchange splitting of the e orbitals, $\Delta_{ex} = 532$ meV, is smaller than the crystal field splitting, $\Delta_{cf} = 694$ meV. For Fe (Co) doped MoS_2, one electron occupies the a defect state and the other one (two) occupy the e_1 spin-up defect state. We obtain $\Delta_{ex} = 650$ meV and $\Delta_{cf} = 704$ meV for $(Mo,Fe)S_2$ and $\Delta_{ex} = 515$ meV and $\Delta_{cf} = 412$ meV for $(Mo,Co)S_2$.

Figure 4(a) shows the DOS of $(Mo,Ni)S_2$ with C_{3v} symmetry. The a state shifts above the e_2 state so that two electrons occupy the e_1 state and two the e_2 spin-up state. However, structure relaxation shows that the symmetry of $(Mo,Ni)S_2$ is reduced to C_1 due to a Jahn-Teller distortion [see Fig. 1(d)]. The energy difference of the C_{3v} and C_1 structures is 383 meV. Due to the Jahn-Teller distortion, we have five a states. Therefore, four electrons occupy the a_1 and a_2 states [see Fig. 4(b)]. All transition metals from the second class, except for Mn, Fe, and Co, show a Jahn-Teller distortion and consequently no magnetism.

Though the binding energy for elements from the third class is lower than for the other two classes (see Fig. 2), $(Mo,X)S_2$ ($X = $ Zn, Cd, Hg) develops magnetism with magnetic moments of $2.0\mu_B$. Figure 4(c) shows the DOS for $(Mo,Zn)S_2$ in C_{3v} symmetry, which is the ground state. The e_1 state is located at the top of the valence band and the a state shifts above the e_2 state. As a consequence, the degenerate e_1 states
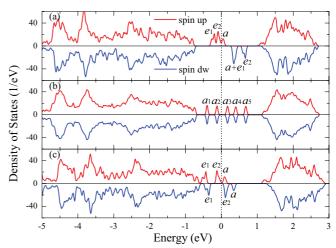

FIG. 3. (Color online) DOS of monolayer MoS_2: (a) Pristine, (b) with two S vacancies, (c) with one Mo vacancy, (d) Sc doped, and (e) Mn doped. The energy axis is calibrated with respect to the core states. The dashed vertical lines indicate the Fermi levels.

FIG. 4. (Color online) DOS of $(Mo,Ni)S_2$ in (a) C_{3v} and (b) C_1 symmetry. (c) DOS of $(Mo,Zn)S_2$ in C_{3v} symmetry.

are occupied by four electrons and two more electrons occupy the e_2 spin-up states. As the impurity states are near the valence bands we obtain p-type doping.

To find the magnetic ground state, both ferromagnetic and antiferromagnetic coupling between the dopants (concentration 6.25%) are considered for the transition metals Mn, Fe, Co, Zn, Cd, and Hg. For Fe and Co doping the antiferromagnetic state is energetically favorable, while Mn, Zn, Cd, and Hg doping results in ferromagnetic ground states, which are 0.02, 3.30, 2.88, and 1.85 meV lower in energy than the respective antiferromagnetic states. An important parameter of a DMS is the Curie temperature (T_C), below which the system develops long range ferromagnetic ordering. We estimate T_C based on the mean-field theory and Heisenberg model using the relation $k_B T_C = (2/3)\Delta E$.[27,28] The results are given in Table I. It has been proposed that the typical T$_C$ for quasi-2D DMS heterostructures (such as Ga$_{1-x}$Mn$_x$As) is far below room temperature ($T_C < 100$ K) based on a disordered Ruderman-Kittel-Kasuya-Yosida (RKKY) lattice field theory.[4,5] Our current results of T_C are consistent with this proposal. For Mn we have repeated the calculations for a smaller dopant concentration of 4% and find a significantly enhanced Curie temperature of $T_C = 92.7$ K.

In conclusion, we have employed first-principles calculations to study the structural, electronic, and magnetic properties of monolayer MoS$_2$ for doping with various transition metals. Our results demonstrate that 2D DMS systems can be realized by this approach. Particularly promising is doping of monolayer MoS$_2$ by Mn, Fe, Co, and Zn. The conclusions obtained for MoS$_2$ should be valid also for other semiconducting transition metal dichalcogenides. Investigation of further materials from this large family therefore is promising to find new 2D DMSs with a high Curie temperature.

*Udo.Schwingenschlogl@kaust.edu.sa

[1] T. Jungwirth, J. Sinova, J. Mašek, J. Kučera, and A. H. MacDonald, Rev. Mod. Phys. **78**, 809 (2006).

[2] K. Sato, L. Bergqvist, J. Kudrnovský, P. H. Dederichs, O. Eriksson, I. Turek, B. Sanyal, G. Bouzerar, H. Katayama-Yoshida, V. A. Dinh, T. Fukushima, H. Kizaki, and R. Zeller, Rev. Mod. Phys. **82**, 1633 (2010).

[3] K. S. Novoselov, A. K. Geim, S. V. Morozov, D. Jiang, Y. Zhang, S. V. Dubonos, I. V. Grigorieva, and A. A. Firsov, Science **306**, 666 (2004).

[4] D. J. Priour, E. H. Hwang, and S. Das Sarma, Phys. Rev. Lett. **95**, 037201 (2005).

[5] E. Z. Meilikhov and R. M. Farzetdinova, Phys. Rev. B **74**, 125204 (2006).

[6] A. V. Krasheninnikov, P. O. Lehtinen, A. S. Foster, P. Pyykkö, and R. M. Nieminen, Phys. Rev. Lett. **102**, 126807 (2009).

[7] B. Huang, H. Xiang, J. Yu, and S.-H. Wei, Phys. Rev. Lett. **108**, 206802 (2012).

[8] Y. Kim, J.-L. Huang, and C. M. Lieber, Appl. Phys. Lett. **59**, 3404 (1991).

[9] J. Heising and M. G. Kanatzidis, J. Am. Chem. Soc. **121**, 11720 (1999).

[10] K. F. Mak, C. Lee, J. Hone, J. Shan, and T. F. Heinz, Phys. Rev. Lett. **105**, 136805 (2010).

[11] A. Kuc, N. Zibouche, and T. Heine, Phys. Rev. B **83**, 245213 (2011).

[12] D. Xiao, G.-B. Liu, W. Feng, X. Xu, and W. Yao, Phys. Rev. Lett. **108**, 196802 (2012).

[13] B. Radisavljevic, J. Brivio, V. Giacometti, and A. Kis, Nat. Nanotechnol. **6**, 147 (2011).

[14] J. N. Coleman, M. Lotya, A. O'Neill, S. D. Bergin, P. J. King, U. Khan, K. Young, A. Gaucher, S. De, R. J. Smith, I. V. Shvets, S. K. Arora, G. Stanton, H.-Y. Kim, K. Lee, G. T. Kim, G. S. Duesberg, T. Hallam, J. J. Boland, J. J. Wang, J. F. Donegan, J. C. Grunlan, G. Moriarty, A. Shmeliov, R. J. Nicholls, J. M. Perkins, E. M. Grieveson, K. Theuwissen, D. W. McComb, P. D. Nellist, and V. Nicolosi, Science **331**, 568 (2011).

[15] Y.-H. Lee, X.-Q. Zhang, W. Zhang, M.-T. Chang, C.-T. Lin, K.-D. Chang, Y.-C. Yu, J. T.-W. Wang, C.-S. Chang, L.-J. Li, and T.-W. Lin, Adv. Mater. **24**, 2320 (2012).

[16] P. Giannozzi, S. Baroni, N. Bonini, M. Calandra, R. Car, C. Cavazzoni, D. Ceresoli, G. L. Chiarotti, M. Cococcioni, I. Dabo, A. D. Corso, S. de Gironcoli, S. Fabris, G. Fratesi, R. Gebauer, U. Gerstmann, C. Gougoussis, A. Kokalj, M. Lazzeri, L. Martin-Samos, N. Marzari, F. Mauri, R. Mazzarello, S. Paolini, A. Pasquarello, L. Paulatto, C. Sbraccia, S. Scandolo, G. Sclauzero, A. P. Seitsonen, A. Smogunov, P. Umari, and R. M. Wentzcovitch, J. Phys.: Condens. Matter **21**, 395502 (2009).

[17] R. M. Martin, *Electronic Structure: Basic Theory and Practical Methods* (Cambridge University Press, Cambridge, UK, 2004).

[18] D. Vanderbilt, Phys. Rev. B **41**, 7892 (1990).

[19] J. P. Perdew, K. Burke, and M. Ernzerhof, Phys. Rev. Lett. **77**, 3865 (1996).

[20] Y. C. Cheng, Z. Y. Zhu, and U. Schwingenschlögl, RSC Adv. **2**, 7798 (2012).

[21] Z. Y. Zhu, Y. C. Cheng, and U. Schwingenschlögl, Phys. Rev. B **84**, 153402 (2011).

[22] T. Cheiwchanchamnangij and W. R. L. Lambrecht, Phys. Rev. B **85**, 205302 (2012).

[23] F. L. Deepak, R. Esparza, B. Borges, X. Lopez-Lozano, and M. Jose-Yacaman, ACS Catal. **1**, 537 (2011).

[24] H. T. Wang, Q. X. Wang, Y. C. Cheng, K. Li, Y. B. Yao, Q. Zhang, C. Z. Dong, P. Wang, U. Schwingenschlögl, W. Yang, and X. X. Zhang, Nano Lett. **12**, 141 (2012).

[25] H.-P. Komsa, J. Kotakoski, S. Kurasch, O. Lehtinen, U. Kaiser, and A. V. Krasheninnikov, Phys. Rev. Lett. **109**, 035503 (2012).

[26] J. J. Palacios and F. Ynduráin, Phys. Rev. B **85**, 245443 (2012).

[27] J. Kudrnovský, I. Turek, V. Drchal, F. Máca, P. Weinberger, and P. Bruno, Phys. Rev. B **69**, 115208 (2004).

[28] F. Máca, J. Kudrnovský, V. Drchal, and G. Bouzerar, Appl. Phys. Lett. **92**, 212503 (2008).